Journal of Applied Polymer Science

Sustained release of potassium diclofenac from a pH-responsive hydrogel based on gum arabic conjugates into simulated intestinal fluid

Adriano V. Reis,[1] Thais A. Moia,[1] Danielly L. A. Sitta,[1] Marcos R. Mauricio,[1] Ernandes T. Tenório-Neto,[1] Marcos R. Guilherme,[1] Adley F. Rubira,[1] Edvani C. Muniz[1,2]

[1]Department of Chemistry, State University of Maringá, CEP 87020-900, Maringá, Paraná, Brazil

[2]Programa De Pós-Graduação Em Biotecnologia Aplicada a Agricultura, Paranaense University (UNIPAR), Umuarama 87502-210, Brazil

Correspondence to: M. R. Guilherme (E-mail: marcos_guilherme@pq.cnpq.br)

ABSTRACT: This work describes the preparation, the swelling properties and the potassium diclofenac (KDF) release profile of hydrogels of gum arabic (GA), *N*′,*N*′-dimethylacrylamide, and methacrylic acid. In order to convert GA into a hydrogel, the polysaccharide was vinyl-modified with glycidyl methacrylate. The hydrogels showed pH-responsive swelling changes, which were more expressive in the basic environment. Release data of KDF were adjusted to a diffusion-based kinetic model that provides an important insight on affinity of the drug for hydrogel and solvent, which may be the leading parameter for release of guest molecules from polymers. The KDF release from the hydrogels into simulated intestinal fluid decreases when the amount of modified GA increases. This was demonstrated to be due to the higher affinity of KDF for GA-richer hydrogel, which makes the anti-inflammatory release less favorable. The analysis of released drug half-time ($t_{1/2} = 16.10$ and 21.51 h) indicated sustained release characteristics. © 2015 Wiley Periodicals, Inc. J. Appl. Polym. Sci. **2016**, *133*, 43319.

KEYWORDS: biomaterials; biomedical applications; drug delivery systems; kinetics; swelling

Received 22 August 2015; accepted 6 December 2015

DOI: 10.1002/app.43319

INTRODUCTION

Hydrogels are made of hydrophilic polymers connected to each other by physical or chemical cross-links. They are capable of absorbing a large volume of water or biological fluids without their tridimensional (3D) structure being dissolved into the liquid.[1–3] The ability to swell in water is due to thermodynamic compatibility of the hydrogel with fluids.[4] These materials are formed of homopolymers or copolymers and their structure may be amorphous, semicrystalline, or hydrocolloidal.

Over the last years, there is an increased interest on controlled release systems,[5–9] owing to development of more potent drugs with high degree of specificity. New approaches on release systems are of essential importance because they provide relevant information both to build strategic synthesis of more advanced materials and to understand their properties, such as transport behavior of drug and water and interaction parameters.

Several mathematical models have been elaborated in an effort to explicate the release mechanisms from water-swellable polymers into aqueous environments. Swelling-based models have been commonly used to determine the release profile of hydrophilic polymers, but they do not provide parameters for affinity of the drug for polymer and solvent. The affinity of the drug for its environment may be the most important parameter in the release of drugs from polymers,[10] although factors such as polymer composition, cross-linking density, hydrogel geometry, degree of swelling, and dissolution and diffusion of solute in the hydrogel, also may contribute to release. Indeed, these factors depend on or are related to physical chemical affinities of the drug for hydrogel and solvent, which may be predicted by the affinity-based models. The comprehension of how the release is affected by the interaction of the drug with hydrogel and surrounding liquid may be used as a design parameter to control the release rate.

Hydrogels combining polysaccharides appear as a biotechnological alternative for a wide variety of applications, including in the controlled release and targeted delivery of drugs.[11–13] Hydrogels that exhibits pH-responsive swelling changes takes advantage for stimuli-triggered release of guest molecules from the polymer. In addition, they are able to preserve the drug against premature degradation or inactivation and deliver it into specific sites of action under a controlled release rate, maximizing the impact on the effective therapy in several treatments as colon-specific diseases.

Table I. Amounts of Substances and KDF in the Hydrogel-Forming Solutions

Substances	H-GAm(75-15-10)	H-GAm(60-30-10)
GAm	3.0 g	2.4 g
DMAAm	0.6 g	1.2 g
MetAc	0.4 g	0.4 g
SPS	2.4 mg	2.4 mg
H_2O	40 mL	40 mL

Gum arabic (GA), also called gum acacia, is an important polysaccharide that has been used in the pharmaceutical formulations, such as controlled release systems,[14–18] and in the food processing, mainly in the sweet products.[19] Here, the choice of GA was made on basis of its wide availability, low toxicity, water solubility, and of its great importance in the several areas of science and (bio)technology.

The use of GA in the preparation of hydrogels as a promising alternative for a variety of applications has attracted much attention. For example, superabsorbent hydrogels of modified GA were shown to be an efficient method for removal of methylene blue and of Pb^{2+} and Cu^{2+} from an aqueous environment.[20,21] Bossoni *et al.* reported the synthesis of hydrogels composed of chemically modified GA and *N*′,*N*′-dimethylacrylamide for controlled release of vitamin B_{12} and potassium diclofenac.[22] In a report by Zohuriaan-Mehr *et al.*, superabsorbent hydrogels were prepared by free radical copolymerization of acrylamide and partially neutralized acrylic acid onto GA.[23] In another report by Reis *et al.*, hydrogels composed of chemically modified GA were demonstrated to be responsive to pH changes.[24] Shaikh *et al.* described the preparation of graft copolymer hydrogels by graft copolymerization of acrylic acid onto GA in the presence of a crosslinking agent.[25] In a research report, Aderibigbe *et al.* prepared GA-based hydrogels by redox cross-linked polymerization for controlled release of *N*-(7-chloroquinolin-4-yl) propane-1,3-diamine and curcumin.[26] In a report by Gerola *et al.*, hydrogel containing curcumin/alpha-cyclodextrin complex were prepared from chemically modified GA for controlled release of curcumin.[27]

The focus of this work is on developing colon-targeting covalent hydrogels based on GA conjugates cross-linked with *N*′,*N*′-dimethylacrylamide (DMAAm) and methacrylic acid (MetAc) for release of guest molecules from water-swellable polymers. Potassium diclofenac (KDF) was used as drug model. KDF is a non-steroidal anti-inflammatory drug used to minimize the inflammation and also as an analgesic drug to reduce the pain.[28] DMAAm and AcMet were used owing to their excellent ability to undergo hydrogelation at conditions that do not affect the structure of the polysaccharide. In addition, they do not undertake hydrolysis at acidic or basic environments, which assures the prevention of the chemical degradation of the hydrogel. For hydrogelation, GA was vinyl-functionalized with glycidyl methacrylate (GMA) using a reaction medium free of potentially toxic reactants. This is found to be an efficient approach to transform uncross-liked polysaccharides, such as GA, into a covalent hydrogel whose cross-links are stable with time, keeping the gel properties.

There are two reaction routes for functionalization of polysaccharides with GMA that have been already reported in the literature: transesterification and epoxy ring-opening mechanisms.[29–31] Although the mechanisms involving reaction of GA with GMA have already been reported, the products resultants from such a reaction have been not yet clearly described and this is beyond identifying transesterification and epoxy ring-opening mechanisms. This information is of great importance because it allows us to go into a detailed discussion of the methacrylate conjugation of GA with GMA. Consequently, the actual composition of hydrogel can be identified. Knowing actual composition of the hydrogel is fundamental to apply a model that takes into account physical chemical interactions of the drug with medium in which it acts. This work deals with an issue of contemporary interest for the development of advanced biomaterials and drug delivery systems. It combines good hydrogel synthesis, studies of the swelling properties of the hydrogel, as well as demonstration of the potential applications of the hydrogel for drug delivery.

EXPERIMENTAL

Materials

Gum arabic, GA (Company-Sudan), glycidyl methacrylate, GMA (Aldrich, USA, ≥97%), *N*′,*N*′-dimethylacrylamide, DMAAm (Aldrich, USA, ≥99%,), hydrochloric acid, HCl (Nuclear, Brazil, 36.5–38%), sodium persulfate, SPS (Vetec, Brazil), methacrylic acid, MetAc (Aldrich, 99%), ethanol (Nuclear, Brazil, 99.5%).

Chemical Modification of GA with Glycidyl Methacrylate (GMA) in Aqueous Solution

GA-modifying solution was prepared with the solubilization of 75 g GA in 500 mL of distilled-deionized water at 65°C. After the mixture was completely homogenized, 0.1*M* hydrochloric acid (HCl) was dropped into the GA solution until a pH 3.5 was reached. Then, 6 mL of GMA were added while stirring and the resultant solution was left to react at 65°C for 12 h. After that, the product (GAm) was precipitated with 1 L of ethanol and subsequently filtrated under reduced pressure. The precipitate was freeze-dried for 12 h.

Preparation of GAm Hydrogel

GAm hydrogel-forming solution was prepared with addition of 15% (w/v) GAm to an aqueous solution consisting of 10 mmol L^{-1} sodium persulfate (SPS). After homogenization, the resultant solution was brought into a glass tube and heated to 75°C for 30 min. After gelation, the hydrogel was washed with distilled-deionized water and left to dry at room temperature. The H-GAm(100) label was used to identify GAm-pure hydrogels.

Preparation of Hydrogel Containing GAm, DMAA, and MetAc

Known amounts of GAm, DMAAm, and MetAc were added to a 10 mmol L^{-1} SPS aqueous solution while stirring. The amounts of the reactants were summarized in Table I. Prior hydrogelation, KDF was added to the hydrogel-forming solution

Figure 1. Photo of dry hydrogels of H-GAm(60-30-10) before (transparent) and after being loaded with KDF (white). The transparent hydrogels were used in the spectroscopic characterization and in the measures of swelling. The white hydrogels, which are loaded with drug, were used in the release experiments. [Color figure can be viewed in the online issue, which is available at wileyonlinelibrary.com.]

to be loaded during the synthesis. The ratio between the mass of KDF and the mass of the reactants corresponded to 20 mg g^{-1} (mg of drug per gram of dry hydrogel). The mixture was transferred to a cylinder glass tube for 30 min at 75°C for hydrogelation. The cylinder-shaped hydrogels were washed with distilled-deionized water for 24 h and left to dry at room temperature. Figure 1 shows a photo of dry hydrogels of H-GAm(60-30-10) before and after being loaded with KDF. Two different hydrogel compositions were prepared with GAm, DMAAm and MetAc: namely, H-GAm(75-15-10) and H-GAm(60-30-10). The (X-Y-Z) label indicates the mass percentages of GAm, DMAAm, and MetAc, respectively, used in the gel formulations. GAm-pure hydrogel (namely, H-GAm(100)) was prepared for reference.

Transmittance FT-IR Spectroscopy

FT-IR spectra of GA, GMA, GAm, and hydrogels were recorded in a Bomen FT-IR model MB100 spectrometer. All the samples were analyzed as powders. Measures were performed in triplicate and a total of 128 scans were run for each spectrum to reach the resolution of 4 cm^{-1}.

^{1}H NMR and ^{13}C NMR Spectroscopies

^{13}C NMR and ^{1}H NMR spectra were recorded in a Varian spectrometer (model Mercury Plus BB) by applying frequencies of 300.059 MHz and 75.457 MHz for the nuclei of ^{1}H and ^{13}C, respectively. D_2O solutions consisting of 0.05% 3-(trimethylsilyl) propionic acid-d_4 sodium salt, as an internal reference, were prepared to acquire the spectra of GA and GAm. The angle pulse and the relaxation time, used for recording the ^{1}H NMR spectra, were fixed in 90° and 30 s, respectively. The signal corresponding to water was suppressed by irradiation during the relaxation. For the ^{13}C NMR, the pulse angle and the relaxed time were 30° and 1 s, respectively. CD_3Cl was used as a solvent for recording the GMA spectra. The chemical shift was given in ppm.

Measures of Swelling Degree (S_w) in Dependence of pH and Ionic Strength (μ)

S_w of the hydrogels was determined by immersing the dry samples of known mass into solutions with different conditions of pH and μ at 37°C. The dry samples were added to aqueous solutions and left to swell until the equilibrium. The hydrogels were removed from the solutions at specific periods and weighed until no weight variation was observed. The influence of μ was studied using sodium chloride solutions. The effect of pH was investigated using buffer solutions. The values of S_w were obtained correlating the water mass within the hydrogel at any time to the initial mass of hydrogel.

Table II. Factors and Levels Selected to Build the 2^2 Full Factorial Design with a Central Point for Swelling Degree of H-GAm(75-15-10) and H-GAm(60-30-10)

			Levels				
Factor	Unity	Type	(−2)	(−1)	(0)	(+1)	(+2)
μ	mol kg^{-1}	Numerical	0.1	0.125	0.15	0.175	0.2
pH		Numerical	2	4	6	8	10

In order to have a deep assessment on the swelling properties, a 2^2 full factorial design with a central point was built. The levels and factors are described in Table II. The time at which the swelling ratio of hydrogel reaches equilibrium depends on its composition, cross-linking degree, polymer density, and so on. Statistical treatment may give an insight important into the swelling properties. The data of S_w were calculated as the average over the three S_w determinations ($n = 3$) for each condition of pH and μ. Design-Expert software (Minneapolis, MN) was used to evaluate the main effects of pH and μ and the interaction effects of pH and μ on S_w.

KDF Release from H-GAm(75-15-10) and H-GAm(60-30-10) Matrices

The tests of release were performed taking into account the statistic treatment of the swelling data. Both of the hydrogels showed larger swelling degrees in the basic environment (as shall be further demonstrated in the results and discussion). Thus, they are suitable to be tested in the simulated intestinal fluid (SIF) in which KDF can be absorbed into blood flow.

SIF was prepared according to the 28th United States Pharmacopeia Convention (USP XXVIII, 2006). The KDF-loaded dry hydrogels were immersed into vessels containing 250 mL of SIF at 37°C and stirred at 50 rpm using a paddle dissolutor (Nova Ética®, Mod. 299). Then, aliquots of 5 mL were collected at specified periods and the absorption readings were made at 271 nm in a UV-Vis spectrophotometer (Shimadzu, UV mini 1240). After the reading, the aliquots were returned to the vessels. The concentrations of KDF released from the hydrogels into SIF were determined from analytical curves correlating the absorbance to the concentration of KDF.

RESULTS AND DISCUSSION

Characterization of GA and GAm by FT-IR Spectroscopy

Only the hydrogels used in the spectroscopic characterization were washed and dried. These hydrogels were not loaded with drug. For characterization, the aim was to find evidences of chemical groups derived from GMA on GAm by spectral changes. In such a case, drug-loaded hydrogel is not required.

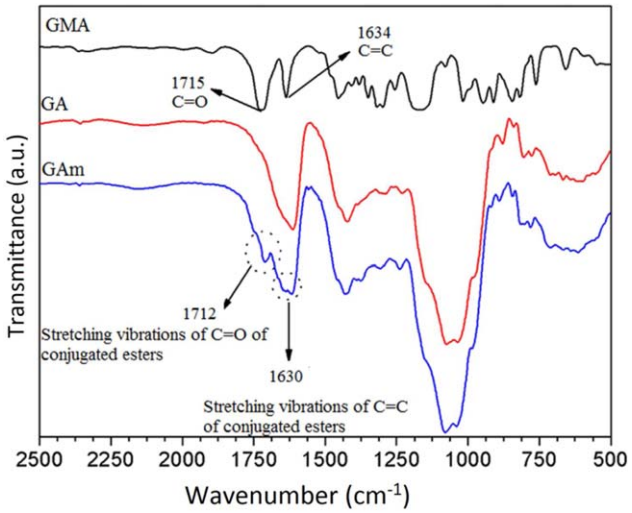

Figure 2. FT-IR spectra of GMA, GA, and GAm. [Color figure can be viewed in the online issue, which is available at wileyonlinelibrary.com.]

Figure 2 shows the FT-IR spectra of GA, GMA and GAm in the spectral scale of 2500 cm^{-1} to 500 cm^{-1}. The band at 1712 cm^{-1} in the spectrum of GAm was attributed to C═O stretching vibrations of conjugated esters issued from GMA. Furthermore, the shift of the band at 1634 cm^{-1} in the spectrum of GMA to 1630 cm^{-1} in the spectrum of GAm was assigned to C═C stretching vibrations of conjugated esters. These findings are strong evidences of the introduction of chemical groups derived from GMA onto GAm.

Characterization of GA and GAm by ^{1}H NMR and ^{13}C NMR Spectroscopies

Figure 3 shows the ^{1}H NMR spectra of GA, GMA, and GAm. The signals at 6.20 and 5.79 ppm in the spectrum of GAm were attributed to vinyl group-linked hydrogen from methacryloyl groups, and the signal at 1.96 ppm was associated to methyl group-linked hydrogen from methacryloyl groups. The signal at 3.32 ppm refers to ^{1}H-resonances from anomeric carbons of 3-methacryloyl-1-glyceryl ester isomer, which is a product of the reaction. The corresponding signal of the glyceryl spacer derived from GMA indicates that GA reacted with GMA by an epoxide ring-opening mechanism.[32]

The chemical modification of GA with GMA was complemented by ^{13}C NMR spectroscopy, shown in Figure 4. The signals of vinyl carbon were detected at 138.52 and 130.41 ppm in the spectrum of GAm. The signals at 172.07 and 20.05 ppm were associated to carbonyl and methyl carbons, respectively. The signals at 60.05 and 56.69 ppm refer to the glyceryl spacer in GAm, which indicate two isomers as the products of reaction: 3-methacryloyl-1-glyceryl ester of gum arabic and 3-methacryloyl-2-glyceryl ester of gum arabic (inset). This evidence is of great significance to confirm the attachment of GMA to GAm by epoxide ring opening mechanism.[32]

Characterization of GAm Hydrogel by FT-IR Spectroscopy

In aqueous solutions with temperatures between 70 and 100°C, SPS is decomposed by a homolytic cleavage to form two sulfate radical ions in the liquid medium.[33] After the breakdown of the initiator, the radical ions attack to vinyl groups from GAm, DMAAm and MetAc. Then the formed macroradicals react with other vinyl molecules in the solution by a radicalar cross-linking/polymerization process, forming hydrogel. Over the radical reaction, the vinyl carbon of conjugated esters in GAm are converted to saturated methyl carbon, resulting in the α,β-unsaturated conjugation-loss of ester groups, as represented in Scheme 1. The conversion of non-conjugated to conjugated esters was characterized by FT-IR spectroscopy.

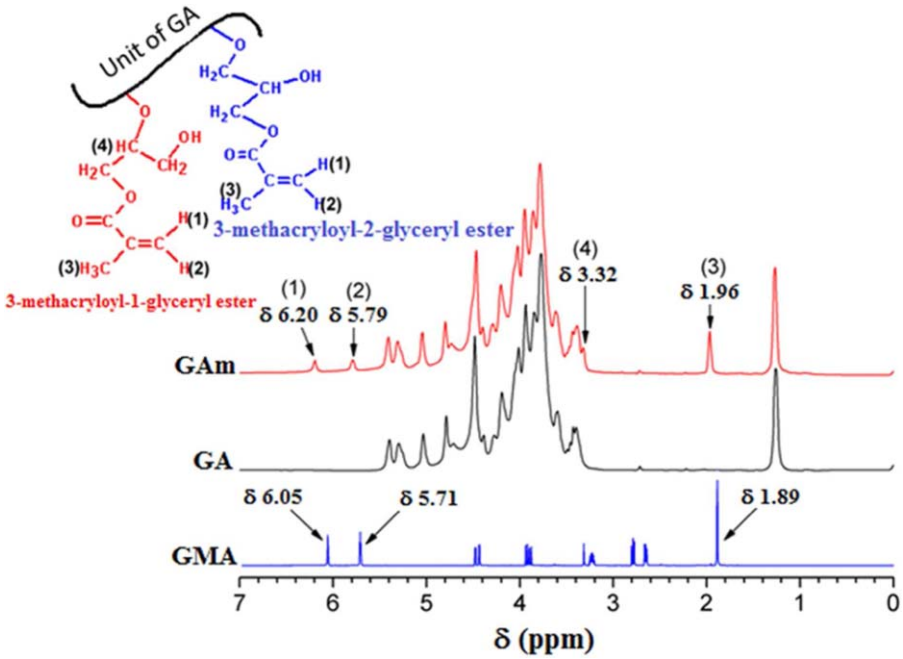

Figure 3. ^{1}H NMR spectra of GA, GAm, and GMA. [Color figure can be viewed in the online issue, which is available at wileyonlinelibrary.com.]

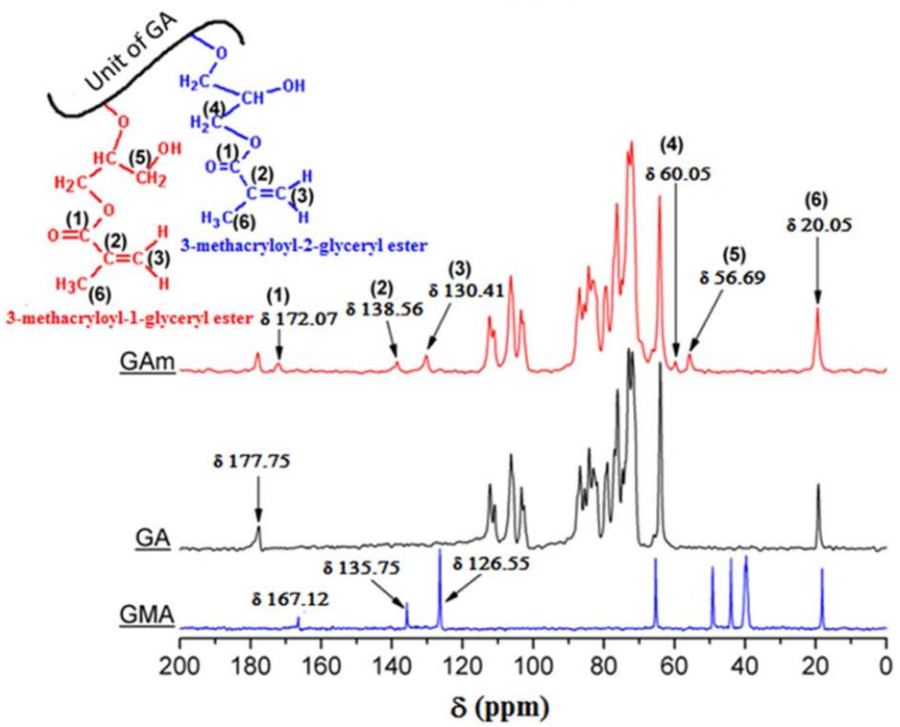

Figure 4. ^{13}C RMN of GA, GAm, and GMA. [Color figure can be viewed in the online issue, which is available at wileyonlinelibrary.com.]

Figure 5 shows the FT-IR spectra of GA, GAm, H-GAm(100), H-GAm(75-15-10) and H-GAm(60-30-10). The band at 1712 cm^{-1} in the spectrum of GAm was attributed to stretching vibrations of carbonyl groups ($\nu C{=}O$) derived from GMA. The shift of this band to 1734 cm^{-1} after the cross-linking/polymerization indicates the α,β-unsaturated conjugation-loss of ester groups, caused by the consumption of vinyl groups in GAm. The broad band at 1728 cm^{-1} was assigned to stretching vibrations of carbonyl groups ($\nu C{=}O$) derived from DMAAm and MetAc moieties in the H-GAm(75-15-10) and H-GAm(60-30-10).

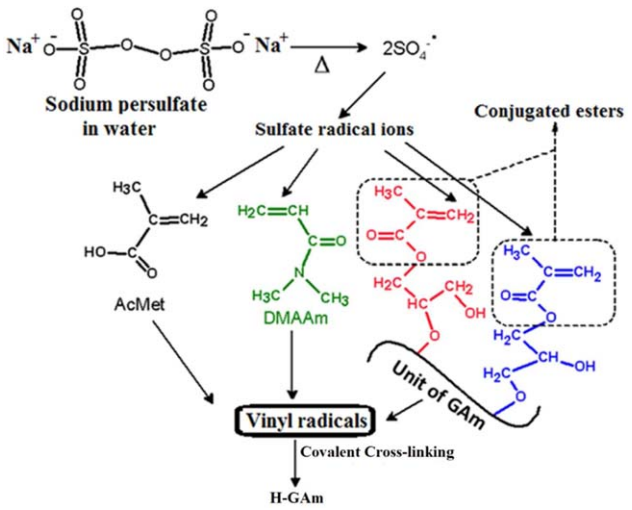

Scheme 1. Proposed mechanism for temperature-induced homolytic cleavage of SPS in water. The radical ions from SPS cleavage attack the vinyl groups from GAm, DMAAm, and MetAc initiating a radicalar polymerization/crosslinking reaction. [Color figure can be viewed in the online issue, which is available at wileyonlinelibrary.com.]

Statistic Treatment for Swelling Degree

The full 2^2 factorial design with a central point for different conditions of pH and μ and the S_w responses are shown in Table III. H-GAm(100) was extremely brittle when submitted to the release tests, even in different swelling stages, and in this particular case, the analysis of this matrix was not taken further. The analyses of variance (ANOVA) for S_w of H-GAm(60-30-10) and H-GAm(75-15-10) were described in Tables IV and V,

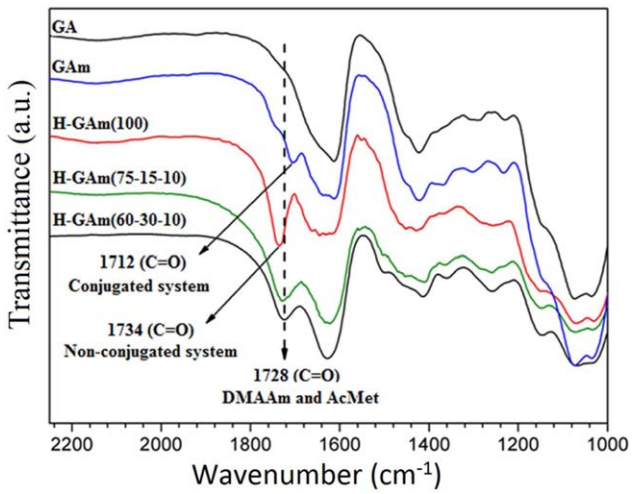

Figure 5. FT-IR spectra of GA, GAm, H-GAm(100), H-GAm(75-15-10), and H-GAm(60-30-10). [Color figure can be viewed in the online issue, which is available at wileyonlinelibrary.com.]

Table III. S_w Responses for H-GAm(60-30-10) and H-GAm(75-15-10) Obtained for the 2^2 Full Factorial Design (Runs 1 to 8) with a Central Point (Runs 9 to 12)

	Factors		Responses	
Runs	pH	μ (mol kg^{-1})	S_w (g/g) H-GAm(60-30-10)	S_w (g/g) H-GAm(75-15-10)
01	4.0 (−1)	0.125 (−1)	6.54	6.79
02	4.0 (−1)	0.175 (+1)	5.23	5.62
03	8.0 (+1)	0.125 (−1)	31.55	29.03
04	8.0 (+1)	0.175 (+1)	25.39	19.85
05	2.0 (−2)	0.150 (0)	4.54	4.13
06	10.0 (+2)	0.150 (0)	39.67	39.95
07	6.0 (0)	0.100 (−2)	15.71	18.46
08	6.0 (0)	0.200 (+2)	12.92	12.14
09 (C)	6.0 (0)	0.150 (0)	13.45	12.51
10 (C)	6.0 (0)	0.150 (0)	13.43	12.47
11 (C)	6.0 (0)	0.150 (0)	13.44	12.43
12 (C)	6.0 (0)	0.150 (0)	13.43	12.39

respectively. The values of the statistic parameter (P) for pH, μ, pH^2, and μ^2, taking into account a confidence interval of 95%, were lesser than 0.001 for both hydrogels. For a value of P lesser than 0.05, the probability for the null hypothesis to be true is lesser than 5%. This indicates that the interaction and the main effects of pH and μ are statically significantly. Furthermore, the lower value of P for the lack of fit suggests a good adjust of the quadratic model to experimental data of S_w.

The adjust of the quadratic model may also be confirmed by the values of R^2, which were 0.9950 for H-GAm(75-15-10) and 0.9971 for H-GAm(60-30-10). Correcting the values of R^2 with respect to the number of freedom degrees, the values of R^2 adjusted are obtained: 0.9909 for H-GAm(75-15-10) and 0.9948 for H-GAm(60-30-10). The data of ANOVA indicate that the quadratic model significantly explicates the experimental data of S_w for both hydrogels.

The effect of μ on S_w was more evident for H-GAm(75-15-10) in the basic medium, which was attributed to the increased ionization degree of this matrix. The larger the ionization degree of the polymer network, the greater the effect of the counter-ions on S_w. H-GAm(60-30-10) presents a larger amount of amide groups that not ionize in the basic environment. In addition, the lower amount of GAm decreases the number of fixed charges, and thus S_w becomes less dependent of counter-ions. In other words, in the basic medium, H-GAm(60-30-10) showed less marked swelling changes in response to μ variation. This clearly suggests that the effect of μ on S_w depends on ionization degree which in turn depends on pH. In summary, the results of ANOVA show that the pH is the most important parameter in S_w and that both hydrogels showed pH-responsive swelling changes, which were more important in the basic environment. Under this condition, S_w increased owing to the greater ionization degree of the hydrogels that causes the polymer network to expand.

Treatment Statistic for Water Transport Mechanism

To gain additional insight into swelling properties, the water transport through the hydrogels was studied. The parameter of water transport was assessed by applying the more general version of the power law equation,[34,35] described by

$$\frac{M_t}{M_{eq}} = kt^n \quad (1)$$

where k is a proportionally constant and n is the diffusional coefficient. M_t and M_∞ are the masses of water absorbed by the hydrogel at a specific time and at equilibrium, respectively.

Table IV. ANOVA Data for the Fit of the Quadratic Model to S_w Data of H-GAm(75-15-10) for the 2^2 Full Factorial Design with a Central Point

Source	Sum of square (SS)	Degree of freedom	Mean squares	*F* value	*P*
pH	932.970	1	932.9698	49,754,303	6.28×10^{-12}
pH^2	114.144	1	114.1437	6,087,165	1.47×10^{-10}
μ	37.826	1	37.8259	2,017,214	7.70×10^{-10}
μ^2	12.135	1	12.1353	647,165	4.24×10^{-9}
pH × μ	17.075	1	17.0750	910,593	2.54×10^{-9}
Lack of fit	5.502	3	1.8338	97,797	5.55×10^{-8}
Pure error	5.63×10^{-5}	3	1.88×10^{-5}		
Total SS	1107.523	11			

Table V. ANOVA Data for the Fit of the Quadratic Model to S_w Data of H-GAm(60-30-10) for the 2^2 Full Factorial Design with a Central Point

Source	Sum of square (SS)	Degree of freedom	Mean squares	*F* value	*P*
pH	1402.285	1	1402.285	5422580	1.75×10^{-10}
pH^2	189.582	1	189.582	733107	3.51×10^{-9}
μ	3.131	1	3.131	12106	1.66×10^{-6}
μ^2	3.290	1	3.290	12724	1.54×10^{-6}
pH x μ	0.101	1	0.101	392	2.82×10^{-4}
Lack of fit	4.515	3	1.505	5819	3.82×10^{-6}
Pure error	7.76×10^{-4}	3	2.59×10^{-4}		
Total (SS)	1608.283	11			

Equation (1) is a semiempirical relation and is valid for first 60% of absorbed water; M_t/M_∞ rate is linear at early times. To understand the water transport mechanism through the cylinder-shaped hydrogels, n should be interpreted as follows: $n = 0.45$, Fickian diffusion; $0.45 < n < 0.89$, anomalous mechanism (contribution of Fickian diffusion and macromolecular relaxation); $n = 0.85$, case II transport (result of macromolecular relaxation of the polymer chains); $n > 0.85$, super case II transport (contribution of macromolecular relaxation and erosion of the polymer chains). The values of n were determined by fitting the experimental data of M_t/M_∞ to eq. (1) for each condition of pH and μ and the results were shown in Table VI. The swelling mechanism for both hydrogels is driven by anomalous transport, $0.45 < n < 0.89$ for any value of pH and μ.

KDF Release from H-GAm(75-15-10) and H-GAm(60-30-10) Matrices

The KDF release from the hydrogels was studied by applying an affinity-based kinetic model that considers the drug release as a result of a partitioning between the solvent phase and the hydrogel.[10,36–38] The occurrence of the partition effect is determined by a α factor, called partition activity, and may be obtained by

$$\alpha = \frac{F_{max}}{1 - F_{max}} \quad (2)$$

where F_{max} is the maximum fractional releases of the drug and α is defined as the ratio of the concentrations of solute between the solvent and the hydrogel phases. The α-parameter expresses the physical chemical affinity of the drug between the hydrogel and solvent phases, thus providing an important insight on affinity of the drug for environment in which it acts. The fractional release (F_R) of KDF was obtained by

$$F_R = \frac{C_{R,t}}{C_0} \quad (3)$$

where $C_{R,t}$ is the concentration of the drug released at a specified time and C_0 is the initial concentration of solute in the hydrogel.

The release constant rate (k_R) was determined by plotting the release kinetics using eq. (4),

$$\frac{\alpha}{2} \ln\left(\frac{F_R - 2F_R F_{max} + F_{max}}{F_{max} - F_R}\right) = k_R t \quad (4)$$

By rearranging eq. (4), yields

$$F_R = \frac{F_{max}\left(e^{2\frac{k_R}{\alpha}t} - 1\right)}{1 - 2F_{max} + e^{2\frac{k_R}{\alpha}t}} \quad (5)$$

Equation (5) is applied for second-order release kinetics. The experimental data were fitted by applying a nonlinear least-squares fitting method with a confidence level of 95%, using Origin© 8.0 software.

Figure 6(a) shows the variations of the concentration of KDF in SIF for H-GAm(75-15-10) and H-GAm(60-30-10) at 37°C as a function of time. By making a relation between the concentration of KDF in SIF and the initial concentration of KDF within the hydrogel, the released amount of the anti-inflammatory can be expressed in terms of fractional release [eq. (3)], as represented in Figure 6(b).

The term F_{max} represents the maximum fraction of released KDF and the term α expresses the partitioning of KDF between the hydrogel and SIF phases. With the normalization, α of KDF may be calculated from F_{max} by eq. (2). Considering that the KDF release from both hydrogels follows a second-order release kinetic, the values of α and F_{max} may be adjusted to eq. (4) and the value of k_R is obtained from angular coefficient of each plot [Figure 6(c)]. Thus, the experimental data may be adjusted to eq. (5). Figure 6(d) shows the experimental data and the fitting

Table VI. n Responses for H-GAm(60-30-10) and H-GAm(75-15-10) Obtained for the 2^2 Full Factorial Design (Runs 1 to 8) with a Central Point (Runs 9 and 10)

	Factors		Responses	
Runs	pH	μ (mol kg^{-1})	*n*, H-GAm (60-30-10)	*n*, H-GAm (75-15-10)
01	4.0 (−1)	0.125 (−1)	0.5279	0.5476
02	4.0 (−1)	0.175 (+1)	0.5246	0.5307
03	8.0 (+1)	0.125 (−1)	0.6108	0.5955
04	8,0 (+1)	0.175 (+1)	0.5750	0.5759
05	2.0 (−2)	0.150 (0)	0.5007	0.5232
06	10.0 (+2)	0.150 (0)	0.6450	0.6475
07	6.0 (0)	0.100 (−2)	0.6362	0.6134
08	6.0 (0)	0.200 (+2)	0.5757	0.5893
09 (C)	6.0 (0)	0.150 (0)	0.6104	0.6006
10 (C)	6.0 (0)	0.150 (0)	0.6109	0.6010

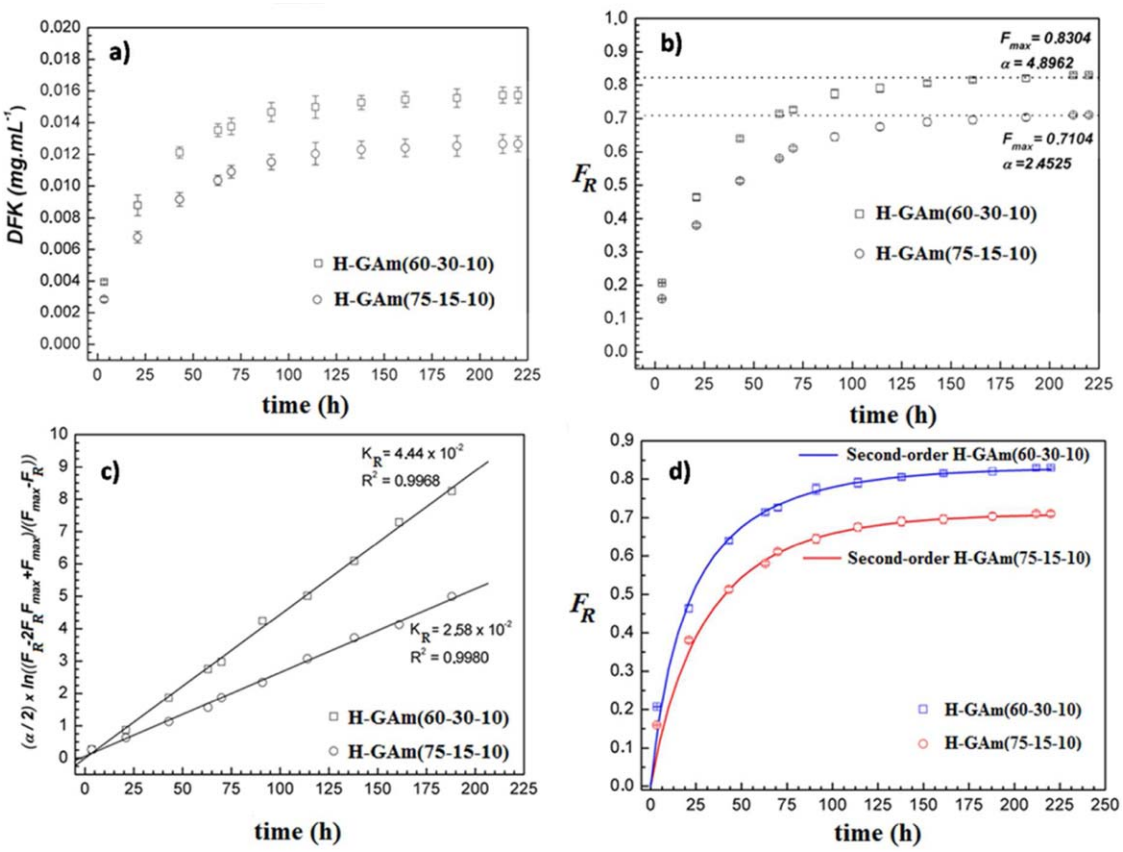

Figure 6. (a) Variations of concentration of KDF in SIF at 37°C as a function of time. (b) Time-dependent fractional release (F_R) of KDF, calculated by eq. (3). (c) Experimental data for time-dependent release of KDF adjusted to eq. (4) (second-order kinetic). (d) Experimental and theoretical data for F_R of KDF adjusted to eq. (5). The continuous lines indicate second-order release kinetics. The circles and squares indicate experimental release data of KDF. [Color figure can be viewed in the online issue, which is available at wileyonlinelibrary.com.]

(continuous lines) through eq. (5) for time-dependent fractional release of KDF from both H-GAm(75-15-10) and H-GAm(60-30-10) into SIF. The fittings confirm the second-order release kinetics, according to eq. (5). The circles and squares indicate experimental release data of KDF.

The released drug half-time ($t_{1/2}$) was determined by eq. (6). $t_{1/2}$ is the time necessary for the concentration of drug in the solvent to reach 50% of F_{max}.

$$t_{1/2} = \frac{\alpha}{2k_R} \ln(3 - 2F_{max}) \quad (6)$$

Table VII summarizes the values of F_{max}, α, k_R, and $t_{1/2}$ for the KDF release from H-GAm(75-15-10) and H-GAm(60-30-10) at 37°C. It is important to highlight that the affinity of the drug for hydrogel increases when α tends to 0.[31] Note that H-GAm(75-15-10), which is the hydrogel with higher concentration of GAm, showed a lower value of α, suggesting a higher affinity of KDF for this hydrogel composition. In such a case, the KDF release into SIF becomes more difficult. This reflects the decrease in the value of k_R, which indicated a slower release rate and consequently a sustained release profile. The analysis of $t_{1/2}$ confirms this argument.

Table VII. Values of F_{max}, α, k_R, and $t_{1/2}$ for KDF Released from H-GAm(75-15-10) and H-GAm(60-30-10) into SIF at 37°C

Hydrogels	F_{max}	A	k_R (h^{-1})	$t_{1/2}$ (h)
H-GAm(60-30-10)	0.8304	4.8962	0.04440	16.10
H-GAm(75-15-10)	0.7104	2.4526	0.02605	21.51

CONCLUSIONS

The current work reported the synthesis and characterization of a polymer hydrogel composed of GA that is covalently linked with MetAc and DMAAm. The mechanism by which GA reacts with GMA was demonstrated by ^{13}C NMR and ^{1}H NMR spectra of GAm. Two isomers that are reaction products resultant of an epoxide ring-opening mechanism were identified: 3-methacryloyl-1-glyceryl ester of GAm and 3-methacryloyl-2-glyceryl ester of GAm. Water transport profiles were extensively studied over a wide range of pH and ionic strength. From those studies, it was found that the hydrogels exhibited pH-responsive structural changes, which were more expressive in the basic environment. The modeling of the release kinetics indicated that the KDF release rate decreases when the amount of GAm in the hydrogel increases. This was related to higher affinity of KDF for hydrogel. The analysis of $t_{1/2}$ suggested sustained release characteristics. This work is of contemporary interest for the development of

advanced biomaterials and stimuli-responsive drug delivery systems.

ACKNOWLEDGMENTS

Authors thank the financial support both from Conselho Nacional de Desenvolvimento Científico e Tecnológico (CNPq), Grant 400702/2012-6, 308337/2013-1, and 167432/2013-3; and from Coordenação de Aperfeiçoamento de Pessoal de Nível Superior (CAPES) and Fundação Araucária.

REFERENCES

1. Buchholz, F. L.; Graham, A. T. *Modern Superabsorbent Polymer Technology*; Wiley-VCH: NY, **1998**.
2. Sadeghi, M.; Hosseinzadeh, H. *J. Appl. Polym. Sci.* **2008**, *108*, 1142.
3. Rodrigues, F. H. A.; Spagnol, C.; Pereira, A. G. B.; Martins, A. F.; Fajardo, A. R.; Rubira, A. F.; Muniz, E. C. *J. Appl. Polym. Sci.* **2014**, *131*, 39725.
4. Peppas, N. A.; Bures, P.; Leobandung, W.; Ichikawa, H. *Eur. J. Pharm. Biopharm.* **2000**, *50*, 27.
5. Ma, L.; Liu, M.; Liu, H.; Chen, J.; Cui, D. *Int. J. Pharm.* **2010**, *385*, 86.
6. Park, M. R.; Chun, C. J.; Cho, C. S.; Song, S. C. *Eur. J. Pharm. Biopharm.* **2010**, *76*, 179.
7. Konishi, M.; Tabata, Y.; Kariya, M.; Hosseinkhani, H.; Suzuki, A.; Fukuhara, K.; Mandai, M.; Takakura, K.; Fujii, S. *J. Controlled Release* **2005**, *103*, 7.
8. Lin, G.; Tarasevich, B. *J. Appl. Polym. Sci.* **2013**, *128*, 3534.
9. Tyagi, P.; Kumar, A.; Kumar, Y.; Lahiri, S. S. *J. Appl. Polym. Sci.* **2011**, *122*, 2004.
10. Lauzon, M. A.; Bergeron, É.; Marcos, B.; Faucheux, N. *J. Controlled Release* **2012**, *162*, 502.
11. You, Y. C.; Dong, L. Y.; Dong, K.; Xu, W.; Yan, Y.; Zhang, L.; Wang, K.; Xing, F. J. *Carbohydr. Polym.* **2015**, *130*, 243.
12. Zhao, Y.; Zhang, X.; Wang, Y.; Wu, Z.; An, J.; Lu, Z.; Mei, L.; Li, C. *Carbohydr. Polym.* **2014**, *105*, 63.
13. Singh, B.; Bala, R. *Int. J. Biol. Macromol.* **2014**, *65*, 524.
14. Ramakrishnan, A.; Pandit, N.; Badgujar, M.; Bhaskar, C.; Rao, M. *Bioresour. Technol.* **2007**, *98*, 368.
15. Banerjee, S. S.; Chen, D. H. *Int. J. Appl. Ceram. Technol.* **2010**, *7*, 111.
16. Nishi, K. K.; Antony, M.; Jayakrishnan, A. *J. Pharm. Pharmacol.* **2007**, *59*, 485.
17. Nayak, A. K.; Das, B.; Maji, R. *Int. J. Biol. Macromol.* **2012**, *51*, 1070.
18. Luo, Y.; Wang, Q. *Int. J. Biol. Macromol.* **2014**, *64*, 353.
19. Leung, A. Y.; Foster, S. Encyclopedia of Common Natural Ingredients Used in Food, Drugs and Cosmetics, 2nd ed.; John: NY, **1996**.
20. Paulino, A. T.; Guilherme, M. R.; Reis, A. V.; Campese, G. M.; Muniz, E. C.; Nozaki, J. *J. Colloid Interface Sci.* **2006**, *301*, 55.
21. Guilherme, M. R.; Reis, A. V.; Paulino, A. T.; Fajardo, A. R.; Muniz, E. C.; Tambourgi, E. B. *J. Appl. Polym. Sci.* **2007**, *105*, 2903.
22. Bossoni, R.; Riul, A.; Valente, A. J. M.; Rubira, A. F.; Muniz, E. C. *J. Braz. Chem. Soc.* **2014**, *25*, 1124.
23. Zohuriaan-Mehr, M. J.; Motazedi, Z.; Kabiri, K.; Ershad-Langroudi, A.; Allahdadi, I. *J. Appl. Polym. Sci.* **2006**, *102*, 5667.
24. Reis, A. V.; Guilherme, M. R.; Cavalcanti, O. A.; Rubira, A. F.; Muniz, E. C. *Polymer* **2006**, *47*, 2023.
25. Shaikh, M. M. M.; Lonikar, M. S.; Lonikar, S. V. *Asian J. Res. Chem.* **2014**, *7*, 407.
26. Aderibigbe, B.; Sadiku, E.; Jayaramudu, J.; Ray, S. S. *J. Appl. Polym. Sci.* **2015**, *132*, 41613.
27. Gerola, A. P.; Silva, D. C.; Jesus, S.; Carvalho, R. A.; Rubira, A. F.; Muniz, E. C.; Borges, O.; Valente, A. J. M. *RSC Adv.* **2015**, *5*, 94519.
28. Brunton, L. L.; Lazo, J. S.; Parker, K. L. In: Skidgel, R. A.; Erdos, E. G. Histamine, Bradykinin, and their Antagonists, 11th ed.; The McGraw-Hill Companies Inc.: NY, **2006**; Chapter 24.
29. Sutter, M.; Siepmann, J.; Hennink, W. E.; Jiskoot, W. *J. Controlled Release* **2007**, *119*, 301.
30. Dijk-Wolthuis, W. N. E.; Kettenes-van den Bosch, J. J.; van der Kerkvan, H. A.; Hennink, W. E. *Macromlecules* **1997**, *30*, 3411.
31. Li, Q.; Wang, D. A.; Elisseeff, J. H. *Macromolecules* **2003**, *36*, 2556.
32. Reis, A. V.; Fajardo, A. R.; Schuquel, I. T. A.; Guilherme, M. R.; Vidotti, G. J.; Rubira, A. F.; Muniz, E. C. *J. Org. Chem.* **2009**, *74*, 3750.
33. Giordano, C. *Acc. Chem. Res.* **1983**, *16*, 27.
34. Costa, D.; Valente, A. J. M.; Miguel, M. G.; Queiroz, J. *Langmuir* **2011**, *27*, 13780.
35. Ritger, P. L.; Peppas, N. A. *J. Controlled Release* **1987**, *5*, 37.
36. Ghosal, K.; Chandra, A.; Rajabalaya, R; Chakraborty, S.; Nanda, A. *Pharmazie* **2012**, *67*, 147.
37. Adnadjevic, B.; Jovanovic, J. *Colloid Surf. B* **2009**, *69*, 31.
38. Reis, A. V.; Guilherme, M. R.; Rubira, A. F.; Muniz, E. C. *J. Colloid Interface Sci.* **2007**, *30*, 128.